Hindawi
Journal of Nanomaterials
Volume 2021, Article ID 9910553, 9 pages
https://doi.org/10.1155/2021/9910553

Research Article

A Novel Polyaniline Nanofiber Combined with Toluidine Blue as a Sensitive Detection Platform for Lignin by Raman Spectroscopy

Hui Zhang, Jing Li, Liang Zhou, and Shengquan Liu

School of Forestry and Landscape Architecture, Anhui Agricultural University, Hefei 230036, China

Correspondence should be addressed to Shengquan Liu; liusq@ahau.edu.cn

Received 22 March 2021; Revised 11 June 2021; Accepted 23 June 2021; Published 26 July 2021

Academic Editor: Tingting Hong

Raman spectroscopy is widely applied in wood science because of its features of being nondestructive, rapidity, and high resolution. However, Raman scattering is weak, and the Raman signal is easily disturbed by autofluorescence arising from endogenous fluorescent molecules in biological tissue. In this work, a sensitive lignin detection platform was fabricated by a composite with a polyaniline (PANI) nanofiber and toluidine blue (TB) under the excitation of visible light. In this platform, TB acts as a specific marker for lignin, and a PANI nanofiber was used as a reinforcing reagent to improve the Raman intensity of TB. When wood slice is impregnated with TB/PANI, the lignin in wood can be precisely labeled with the TB, and the Raman intensity of TB had a threefold increase at 532 nm excitation. This TB/PANI detection platform is expected to make a significant contribution in qualitative and quantitative analysis of lignin to avoid autofluorescence in various lignin-based biosciences.

1. Introduction

Lignin is a major component of the cell wall in wood; the content of lignin has a significant effect on wood performance; for example, lignin in plant fibers is generally regarded as undesirable by the pulp and paper industry, but the high concentration of lignin in the middle lamella between cells in wood is regarded as a positive benefit; thus, the determination of lignin quantity is very important in wood science [1]. Many standard methods for biomass analysis such as wet chemical techniques [2] and analytical techniques such as high-performance liquid chromatography (HPLC) [3], gas chromatography (GC) [4], and nuclear magnetic resonance (NMR) [5] are laborious and slow and employ a variety of harsh reagents requiring some degree of remediation [6].

Raman spectroscopic imaging has been increasingly used in the field of wood science for its ability to characterize various chemical compositions in wood cell walls with minimal sample preparation and provide spatial and spectral information about a sample simultaneously [7]. For instance, the structural characterizations of lignin and the chemical transformations of lignin have been studied by using a confocal Raman microscope [8]. Unfortunately, this is not often achieved in practice when using UV/visible laser excitation to measure biomass as the autofluorescence arises from endogenous fluorescent molecules in biological tissues which makes it difficult to obtain Raman spectra with an acceptable signal-to-noise ratio [9]. Lignin has strong autofluorescence with ultraviolet (UV), blue, green, and red light excitation [10]. To exploit the sensitivity and quantitative detection of lignin, it is necessary to introduce some markers of lignin without an autofluorescence background in Raman spectroscopic imaging. Toluidine blue (TB) is a polychromatic stain, which can be used to differentiate lignified tissues from nonlignified tissues [11–13].

However, the sensitivity of Raman spectroscopy is somewhat poor as only a small number of incident laser photos are elastically scattered. To overcome this problem, many special Raman signal-enhancing techniques have been studied extensively [14]. Polyaniline (PANI) is a conducting polymer which has been utilized in a wealth of devices including secondary batteries and microelectronics [15–18], and it was also widely used in Raman spectra and can act as solid

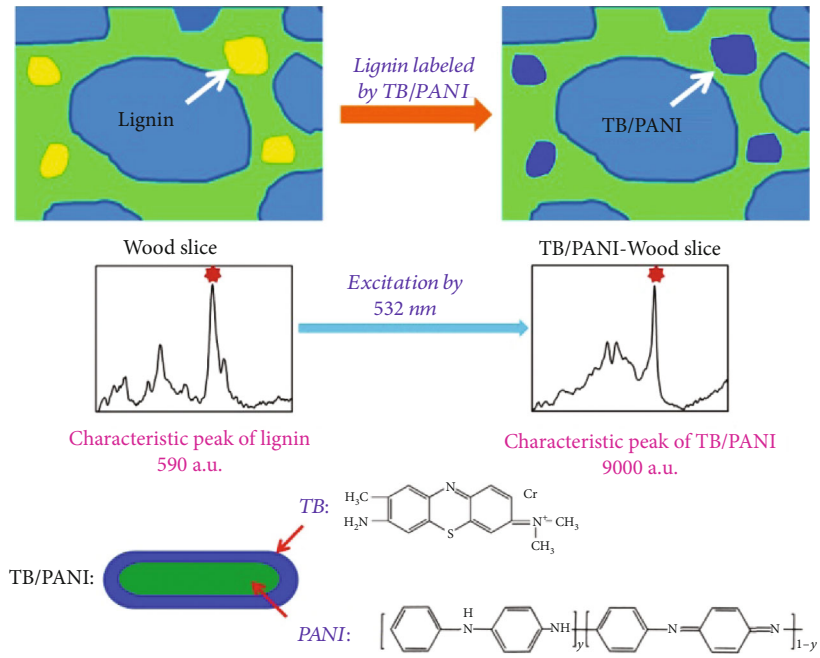

Scheme 1: Schematic illustration of lignin in wood detected by the TB/PANI platform.

supporting material in the design of different surface-enhanced Raman scattering (SERS) substrates [19, 20].

Herein, we have prepared a PANI nanofiber and combined TB together for the sensitive detection of lignin in wood slice. In this platform, TB was chosen as a sensitive and specific biomarker for lignin, and the PANI nanofiber can improve the Raman intensity of TB. First, TB/PANI was assembled on wood slice by the impregnation method. Second, in the presence of target lignin, it would be labeled with TB and a powerful Raman signal was obtained by the approach between PANI and TB at the excitation wavelengths of 532 nm. This TB/PANIA platform had high specificity and sensitivity and can quantitatively detect lignin to avoid autofluorescence stimulated by the visible range light. The strategy of this detection system is shown in Scheme 1. This system has characteristics of simple preparation process, low cost, and being nondestructive and may be an effective detection method for lignin-based materials.

2. Experiment

2.1. Materials. All of the reagents including aniline, TB, p-toluene sulfonic acid (PTS), ammonium persulfate (APS), ethanol, and cyclohexane are of analytical grade. They were used in experiments without further purification. Deionized water was used throughout the experiment to prepare the solutions.

2.2. Preparation of TB/PANI. PANI was synthesized by using 0.5 g aniline, 0.01 g PTS, and 0.5 g APS in cyclohexane/water solution at room temperature. After magnetic stirring for 24 h, the mixture was washed with ethanol several times to remove the reaction byproducts; the dark green-colored PANI solution with a solid content of 2% was collected for further experiments. The TB/PANI was prepared by adding PANI to 2 mmol/L TB aqueous solution treated ultrasonically for 15 min. Experiments were performed with TB : PANI volume ratios of 1 : 1, 2 : 1, and 3 : 1, to understand the influence of PANI content on the Raman intensity of TB.

2.3. Preparation of TB/PANI/Wood Slice. Wood slices were taken from an 8-year-old normal wood of *poplar 107*, the wood was immersed in water for 24 h for softening, and 20 μm thick sections were cut on a rotary microtome (LEICARM2265). The wood slices were immersed into TB/PANI in a sealed dish under ultrasonic vibration (40 W in power) for 30-60 min.

2.4. Characterization. FTIR spectra of samples were collected with a BRUKER TensorII Fourier transform infrared spectrometer (America). The samples were analyzed using a diamond ATR accessory. The phase structure and purity of the samples were examined by X-ray diffraction (XRD) using a XRD-3 (PUXI, China) with a diffractometer with Cu Kα radiation (λ = 1.54 Å) at a scanning rate of 2o/min. The morphology of the samples was carried out on a SEM instrument (Hitachi S-4800, Japan). The UV-vis absorbance was measured by using a UV-1800 spectrophotometer (analytic JENA, S600, Germany). The detection performance obtained using the TB/PANI-wood slice was assessed in conjunction with a Raman spectrometer (Thermo Fisher, America) equipped with a 40x objective lens. Wood slices were impregnated with TB (Figure 1)(a) and PANI (Figure 1(b)) for 24 hours. Before the Raman test, impregnated slices were rinsed with deionized water. The wavelength of the excitation laser was 532 nm, and the laser power and integration time were set at 5.0 mW and 10 s, respectively. For mapping, an integration time of 1 s and 0.17 mm steps were chosen and every pixel corresponds to one scan. For comparison, TB-impregnated filter paper, degreasing cotton, and wood slice treated with

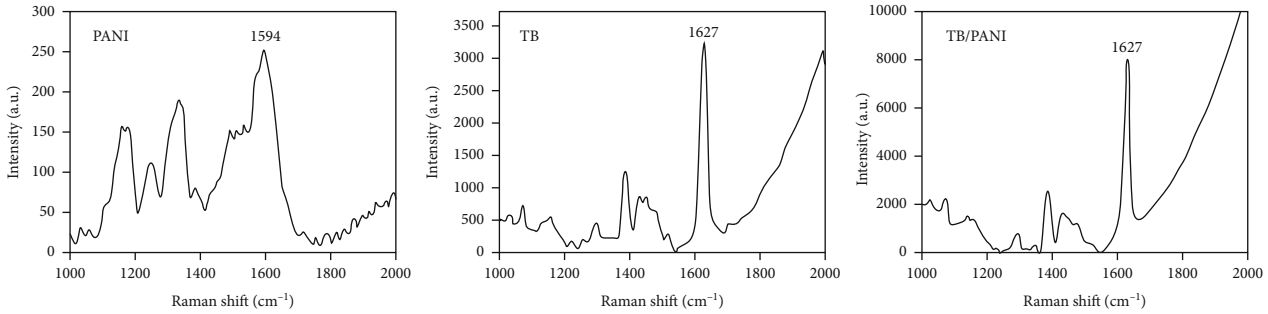

Figure 1: Raman characterization of PANI, TB, and TP/PANI.

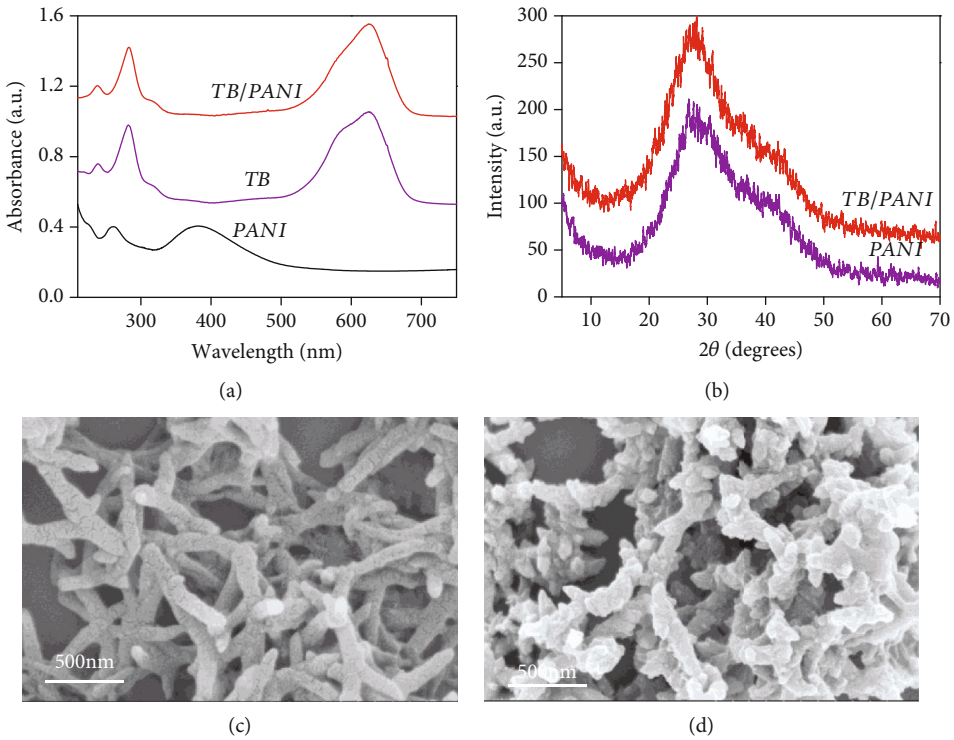

Figure 2: UV-vis spectra of TB, PANI, and TB/PANI (a), XRD images of PANI and TB/PANI (b), and SEM images of PANI (c) and TB/PANI (d).

TB/polyglycol diglycidyl ether resin were also tested with a Raman spectrometer using the same method.

3. Results and Discussion

The TB/PANI was prepared by the ultrasonic-assisted impregnation method; ultrasonic vibrations in a liquid create pressure waves, resulting in the formation, growth, and implosion of millions of microscopic bubbles [21]. This creates extreme pressures, temperatures, and cooling rates at the implosion sites which can make TB achieve better dispersion on the PANI surfaces.

The UV-vis absorption spectra of PANI show photoadsorption at the wavelengths of 265 and 385 nm. While PANI is mixed with TB, the UV-vis adsorption is 281 and 625 nm (Figure 2(a)). Figure 2(b) shows XRD patterns of PANI and TB/PANI. The XRD pattern of the PANI exhibits major reflection peaks at $2\theta = 27°$, and similar peak appeared in the sample of TB/PANI. The XRD study showed that crystallinities of PANI were high, and the addition of TB does not change the crystal type of PANI. The PANI nanofibers typically have diameters of about 70 nm and are up to 500 nm in length (Figure 2(c)). After PANI was mixed with TB, the TB/PANI had the similar morphology, while the surface became rough (Figure 2(d)). The above results show that the compatibility between TB and PANI was very good.

XRD patterns of wood slice and wood slice impregnated with TB (2 mM), PANI, and TB/PANI (volume ratio of 2 : 1) are presented in Figure 3(a). The diffraction peak at about 22° was believed to represent the crystalline region of the cellulose in wood slice. No other new diffraction peaks were found in the sample of TB-wood slice; it might be seen that there was good compatibility and interaction between wood slice and TB. The diffraction peak of PANI-wood slice

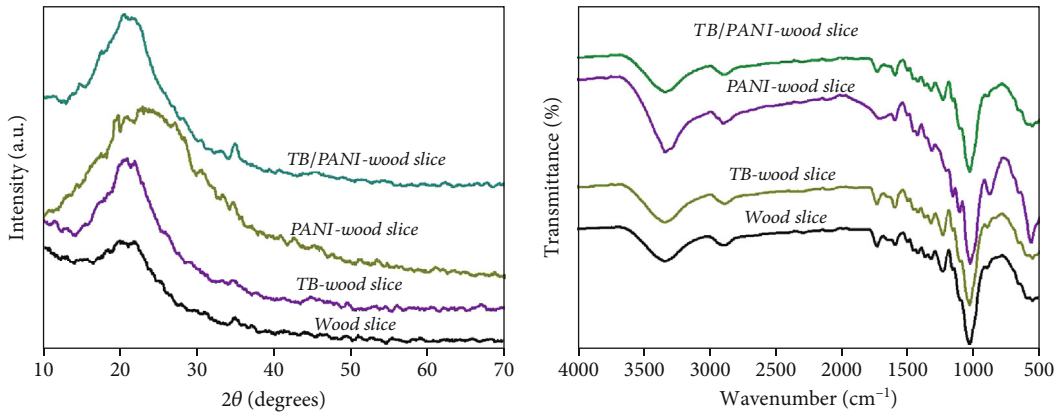

Figure 3: XRD images of wood slice and TB/PANI/wood slice (a) and FTIR images of wood slice, PANI-wood slice, TB-wood slice, and TB/PANI-wood slice (b).

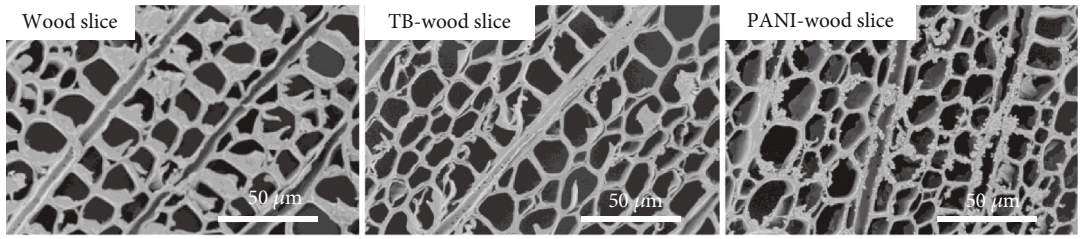

Figure 4: SEM images of wood slice, TB-wood slice, and PANI-wood slice.

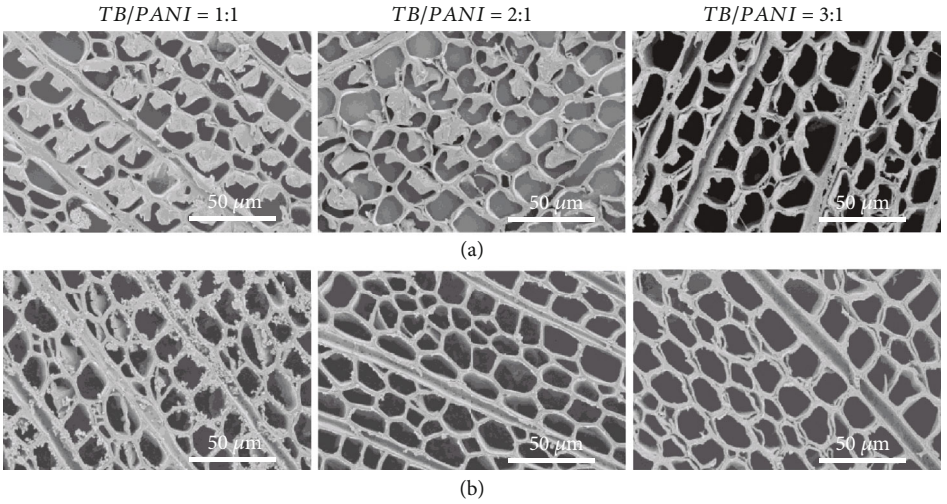

Figure 5: SEM image of wood slice treated with TB/PANI at the volume ratio of 1 : 1, 2 : 1, and 3 : 1 after ultrasonic dispersion 30 min (a) and 60 min (b).

gets broadened from 22° to 27°, and there were only diffraction peaks at 22° with the sample of TB/PANI-wood slice; maybe the lower content of PANI showed better compatibility with wood slice. The FTIR spectra of wood slice, PANI-wood slice, TB-wood slice, and TB/PANI-wood slice can be seen in Figure 3(b). A strong hydrogen-bonded O-H stretching absorption around 3340 cm^{-1} and a prominent C-H stretching absorption around 2900 cm^{-1} were found. In the region from 1700 to 900 cm^{-1}, many discrete absorption bands due to various functional groups present in wood constituents are observed [22]. The strength of the absorption peaks at 3330 cm^{-1} was slightly diminished which may be attributed to the intermolecular hydrogen bonding between the PANI and wood slice. These evidences indicated that there was no new chemical bond and the main interaction in these samples was physical.

The morphology of the wood slice, TB-wood slice, and PANI-wood slice was observed using SEM (Figure 4). All the samples were treated by ultrasonic dispersion for 30 min prior to the test. The wood vessels with the diameter

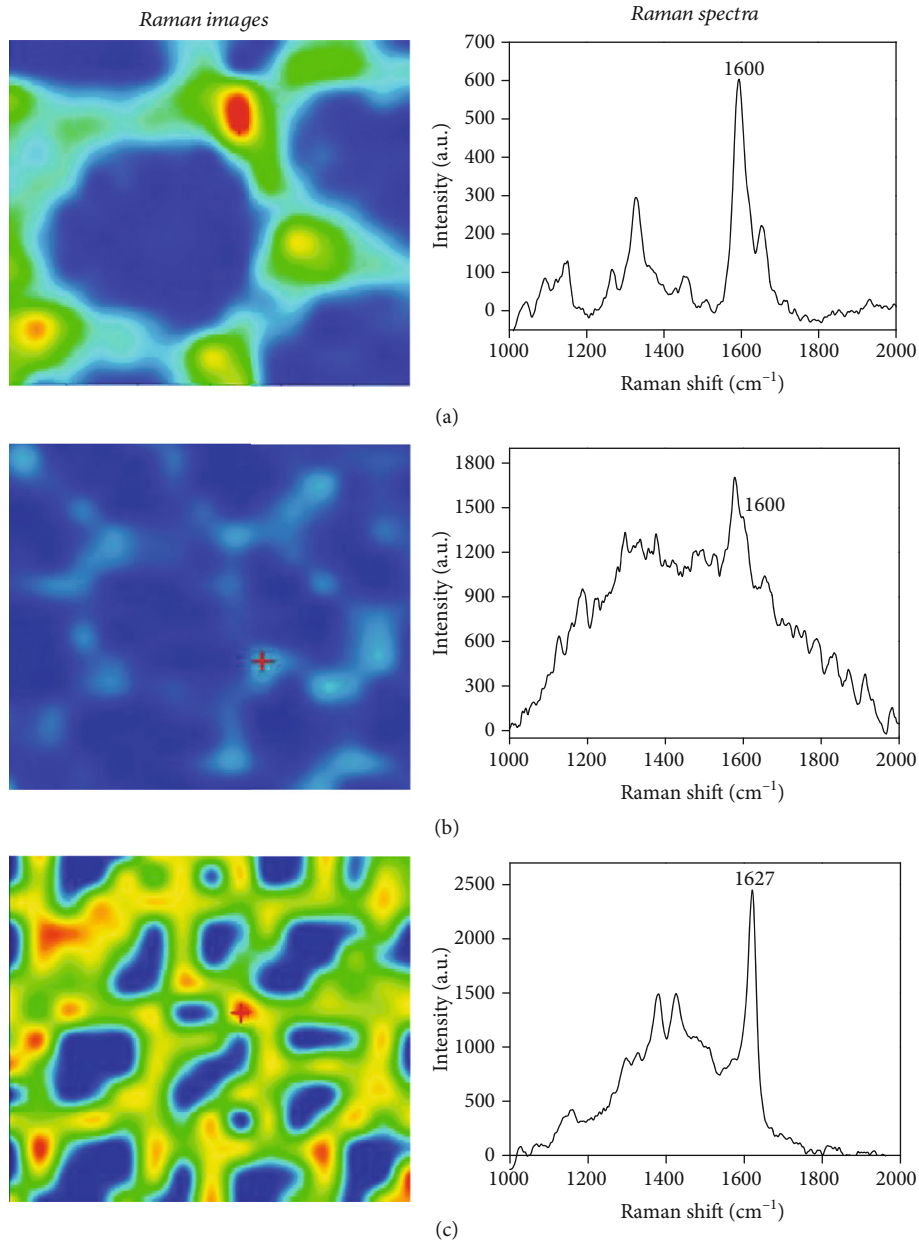

Figure 6: Raman characterization of wood slice (a), PANI-wood slice (b), and TB-wood slice (c).

of about 10-20 μm are irregularly circular, which could be clearly observed. The wood structure has not obviously changed after the treatment with TB, but the surface of PANI-wood slice was coarse; the PANI mainly fills in wood macrospaces as wood cell lumen, is adsorbed on the wood cell wall surface, and enters into the pit chamber in the wood cell wall.

When the wood slice was impregnated with TB/PANI (ratio of 1 : 1, 2 : 1, and 3 : 1) under ultrasonic dispersion for 30 min, the wood slice structure commendably remained. Aggregation disappears in the samples at different volume ratios of TB to PANI (Figure 5(a)). Similar trends were observable in wood slices treated under ultrasonic dispersion for 60 min (Figure 5(b)), and the surface of the wood slices is smooth and clean; therefore, the ultrasonic time was 60 min which was chosen in the follow-up experiment. These results indicated that the compatibility between TB/PANI and wood slice was good.

The fabrication process of the detection platform was characterized by using a Raman spectrometer; when the concentration of TB was 1.0, 2.0, and 3.0 mM, the difference of Raman intensity is not great, which ranges from 3000 to 4000; thus, 2.0 mM TB was used in this detection platform. The Raman peak of 1627 cm^{-1} and 1594 cm^{-1} belongs to TB and PANI, when the TB was mixed with PANI (volume ratio of 2 : 1), the peak shape of TB/PANI had the same trends with the TB, and the peak intensity of 1627 cm^{-1} was increased from 3000 to 8000 (Figure 1(c)); the proposed detection platform would achieve significant improvement for the detection of lignin.

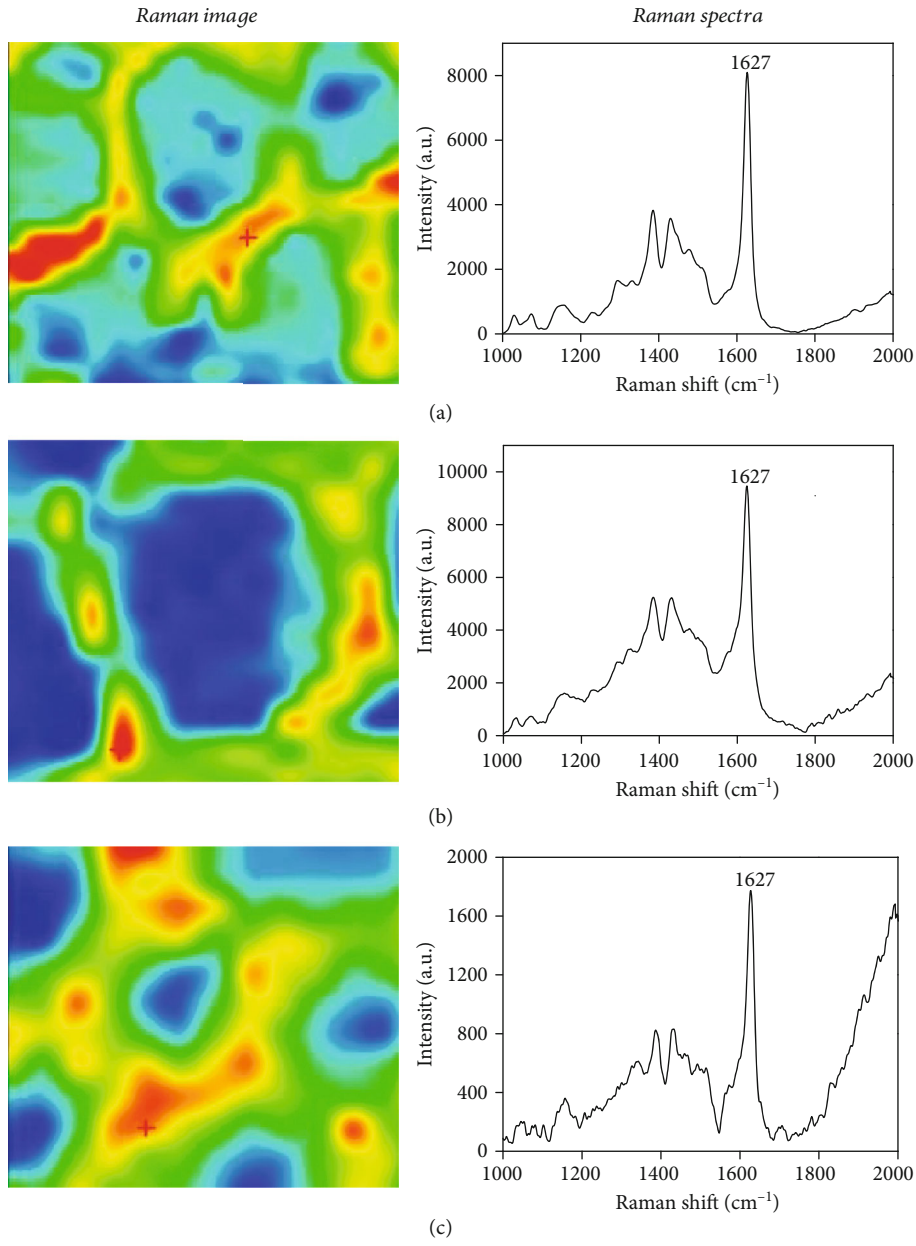

Figure 7: Raman characterization of wood slice with the TB/PANI volume ratio of 1 : 1 (a), 2 : 1 (b), and 3 : 1 (c).

Figure 6(a) shows the Raman signal responses of wood slice, lignin was mainly located in the cell corner of wood slice [23], which showed a characteristic peak at 1600 cm^{-1}, and the maximum intensity of this peak is 600. The peak intensity of 1600 cm^{-1} gradually increased to 1800 after the wood slice was impregnated with PANI (Figure 6(b)), but the wood slice emits strong autofluorescence which interferes with the experiment sensitivity of the determination of lignin. The Raman spectra of wood slice impregnated with TB are shown in Figure 6(c), the peak intensity at 1627 cm^{-1} which was attributed to TB was 2500, similar to lignin in wood slice, and TB was mainly seen in the cell corner. Furthermore, compared with wood slice treated with PANI, TB-wood slice had a little fluorescent background; therefore, the peak at 1627 cm^{-1} was chosen as the standard to judge the Raman signal intensity and the concentration of lignin in this work.

To study the analytical ability and real sample detection potential of the proposed TB/PANI platform, Raman characterization of wood slice treated with TB/PANI at various volume ratios was investigated. The Raman images showed the strongest peak of 1627 cm^{-1} in the cell corner, which were representative of lignin. The Raman intensity was 8000 at 1627 cm^{-1} when wood slice was treated with TB/PANI at a volume ratio of 1 : 1 (Figure 7(a)); when the volume ratio of TB/PANI was changed to 2 : 1, the Raman intensity was increased to 10000 (Figure 7(b)), but the Raman intensity decreased to 1700 when the ratio of TB/PANI reaches 3 : 1 (Figure 7(c)); it may be attributed to the viscosity of TB/PANI that increased with the increase in TB in the mixture; thus, it is

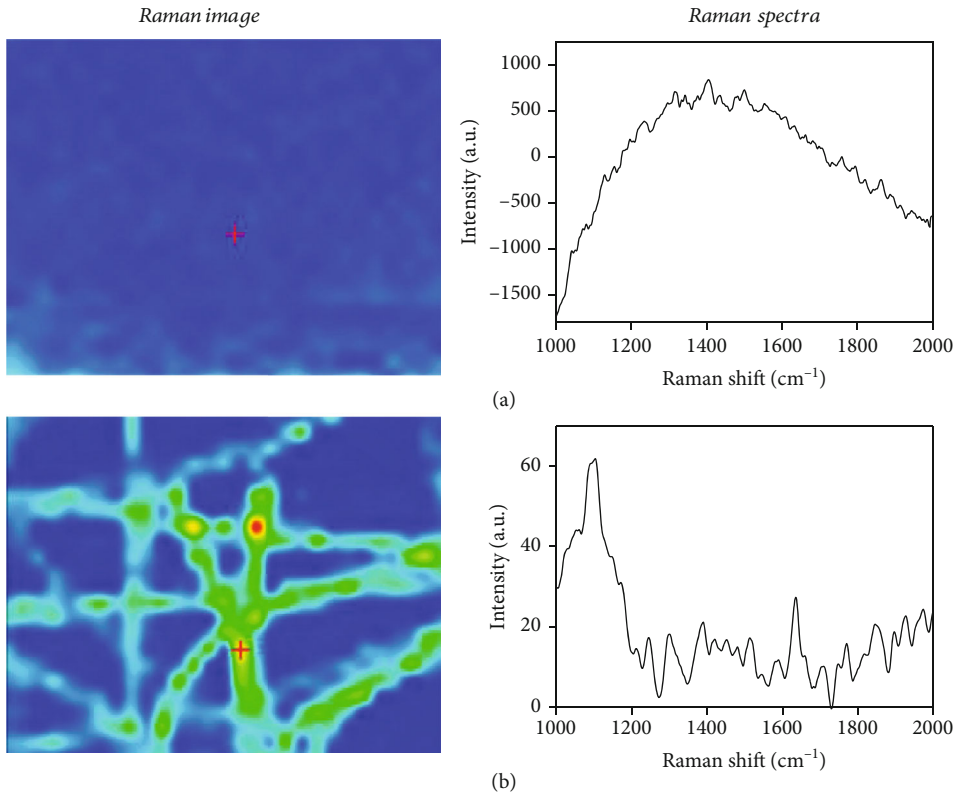

Figure 8: Raman characterization of the filter paper (a) and degreasing cotton (b).

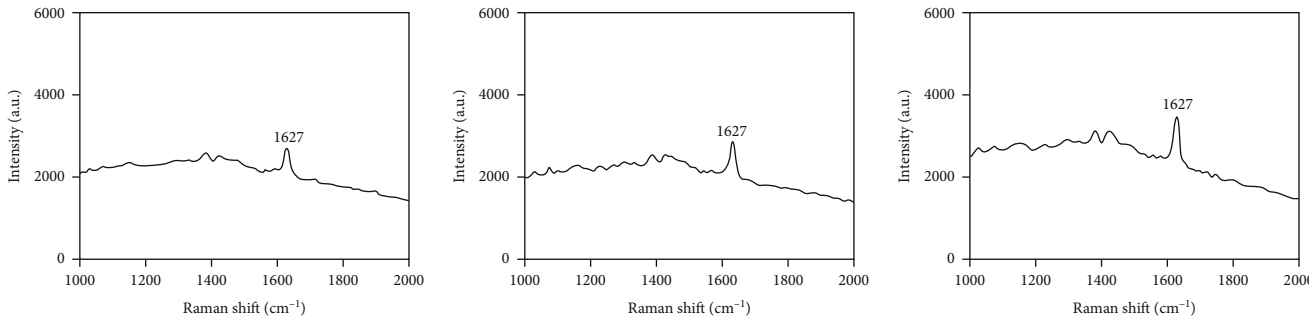

Figure 9: Raman characterization of wood slice with the TB/DER736 volume ratio of 1 : 1 (a), 2 : 1 (b), and 3 : 1 (c).

difficult to enter into the wood cell wall. These results implied that TB/PANI is suitable as an accurate and specific detection platform for the analysis of lignin, and the proper ratio of TB/PANI is 2 : 1, which was thus adopted in this work.

To further determine whether the TB can act as a sensitive and specific biomarker for lignin, a filter paper and degreasing cotton which has no lignin were chosen as control samples. When the filter paper was treated with TB, no characteristic peaks of the TB (1627 cm^{-1}) appeared (Figure 8(a)), and the similar phenomena were found in the sample of degreasing cotton; when it was incubated with TB, only weak signals of TB can be observed in Figure 8(b), because only a small amount of TB adheres to the interior of the cotton fiber. These results suggest that TB had the selective recognition of lignin, and it can act as a lignin marker.

The techniques for enhancing the Raman signals are mainly based on resonant Raman scattering (RRS) or surface-enhanced Raman scattering (SERS). For RRS, the resonance state arises when the excitation wavelength was resonant with a molecular transition. As for SERS, the two widely accepted mechanisms are the electromagnetic mechanism (EM) and chemical mechanism (CM). Briefly, the EM field is enhanced by the excitation of localized surface plasmon resonance when light interacts with metals [24]. CM is based on a charge transfer between the molecule and the substrate, and the polarizability of the molecule increases; therefore, the cross section of the Raman scattering increases. In our work, RRS and EM are not likely, while CM is possible. The PANI nanofiber has certain conductivity doped with protonic acid, and the basic structure of TB is similar to that

of PANI, so that charge transfer could easily occur as TB contacts close to PANI.

To testify this hypothesis, Raman characterization of wood slice treated with TB and nonconductive polyglycol diglycidyl ether resin (DER736) is shown in Figure 9. After wood slice was impregnated with TB/DER736, the Raman intensity showed little variation at the volume ratios of 1 : 1, 2 : 1, and 3 : 1. The maximum Raman intensity is about 2890 when the ratio of TB/PANI reaches 3 : 1, indicating that the addition of TB/DER736 did not enhance the Raman intensity of lignin in wood slice compared with TB/PANI.

These observations suggest that the CM dominates over the surface-enhanced effect in this study, charge transfer can occur between PANI and TB, and the similarity of the chemical structure between PANI and TB may be another factor contributing to the Raman enhancement.

4. Conclusions

In this study, a TB/PANI platform was prepared for the sensitive detection of lignin in wood slice. The PANI nanofiber was a potent enhancer to improve the Raman intensity of TB which acts as a marker of lignin in wood slice. At the 532 nm excitation, Raman intensity of TB could be improved more than three times to avoid autofluorescence. This lignin-recognizing platform could be utilized to proffer researchers a versatile, nondestructive, noninvasive, high-throughput analytical tool. In view of these advantages, we anticipate that this highly sensitive and selective method has potential to be applied to the lignin-based material area.

Data Availability

The data used to support the findings of this study are available from the corresponding author upon request.

Conflicts of Interest

The authors declare that there is no conflict of interest regarding the publication of this paper.

Authors' Contributions

Hui Zhang, Liang Zhou, and Shengquan Liu conceived and designed the experiments. Hui Zhang and Jing Li performed the experiments. Liang Zhou and Jing Li analyzed the data. Hui Zhang and Jing Li wrote the paper. Liang Zhou and Shengquan Liu have given their approval for the final version of the manuscript. Hui Zhang and Jing Li contributed equally to this work.

Acknowledgments

The work was supported by the National Key R&D Program of China (2017YFD0600201), Postdoctoral Science Foundation of Anhui Province (2019B316), and Science and Technology Project of Education Department of Anhui Province (KJ2019A0200).

References

[1] L. Donaldson, J. Hague, and R. Snell, "Lignin distribution in coppice poplar, linseed and wheat straw," *Holzforschung*, vol. 55, no. 4, pp. 379–385, 2001.

[2] J. S. Lupoi, S. Singh, R. Parthasarathi, B. A. Simmons, and R. J. Henry, "Recent innovations in analytical methods for the qualitative and quantitative assessment of lignin," *Renewable & Sustainable Energy Reviews*, vol. 49, pp. 871–906, 2015.

[3] S. R. Decker, A. E. Harman-Ware, R. M. Happs et al., "High throughput screening technologies in biomass characterization.," *Frontiers in Energy Research*, vol. 6, 2018.

[4] Y. Lu, X. Y. Wei, J. P. Cao et al., "Characterization of a bio-oil from pyrolysis of rice husk by detailed compositional analysis and structural investigation of lignin," *Bioresource Technology*, vol. 116, pp. 114–119, 2012.

[5] H. M. Wang, C. Y. Ma, H. Y. Li, T. Y. Chen, and R. C. Sun, "Structural variations of lignin macromolecules from early growth stages of poplar cell walls," *ACS Sustainable Chemistry & Engineering*, vol. 8, pp. 1813–1822, 2019.

[6] J. S. Lupoi, S. Singh, B. A. Simmons, and R. J. Henry, "Assessment of lignocellulosic biomass using analytical spectroscopy: an evolution to high-throughput techniques," *Bioenergy Research*, vol. 7, no. 1, pp. 1–23, 2013.

[7] X. Zhang, Z. Ji, X. Zhou, J. Ma, and F. Xu, "Method for automatically identifying spectra of different wood cell wall layers in Raman imaging data set," *Analytical Chemistry*, vol. 87, pp. 1344–1350, 2014.

[8] Y. Xia, T. Y. Chen, J. L. Wen, Y. L. Zhao, J. Qiu, and R. C. Sun, "Multi-analysis of chemical transformations of lignin macromolecules from waterlogged archaeological wood," *International Journal of Biological Macromolecules: Structure, Function and Interactions*, vol. 109, pp. 407–416, 2018.

[9] S. Diao, G. Hong, A. L. Antaris et al., "Biological imaging without autofluorescence in the second near-infrared region," *Nano Research*, vol. 8, no. 9, pp. 3027–3034, 2015.

[10] R. Decou, H. Serk, D. Ménard, and E. Pesquet, "Analysis of lignin composition and distribution using fluorescence laser confocal microspectroscopy," *Methods in Molecular Biology*, vol. 1544, pp. 233–247, 2017.

[11] H. P. S. Abdul Khalil, M. Siti Alwani, R. Ridzuan, H. Kamarudin, and A. Khairul, "Chemical composition, morphological characteristics, and cell wall structure of Malaysian oil palm fibers," *Polymer-Plastics Technology and Engineering*, vol. 47, no. 3, pp. 273–280, 2008.

[12] G. Siqueira, A. M. F. Milagres, W. Carvalho, G. Koch, and A. Ferraz, "Topochemical distribution of lignin and hydroxycinnamic acids in sugar-cane cell walls and its correlation with the enzymatic hydrolysis of polysaccharides," *Biotechnology For Biofuels*, vol. 4, no. 1, p. 7, 2011.

[13] D. Saxena and G. Stotzky, "Bt corn has a higher lignin content than non-Bt corn," *American Journal of Botany*, vol. 88, no. 9, pp. 1704–1706, 2011.

[14] S. Cong, Y. Yuan, Z. Chen et al., "Noble metal-comparable SERS enhancement from semiconducting metal oxides by making oxygen vacancies," *Nature Communications*, vol. 6, no. 1, p. 7800, 2015.

[15] R. J. Zeng, Z. Luo, L. Zhang, and D. Tang, "Platinum nanozyme-catalyzed gas generation for pressure-based bioassay using polyaniline nanowires-functionalized graphene oxide framework," *Analytical Chemistry*, vol. 90, no. 20, pp. 12299–12306, 2018.

[16] B. Zhang, Y. He, B. Liu, and D. Tang, "Nickel-functionalized reduced graphene oxide with polyaniline for non-enzymatic glucose sensing," *Microchimica Acta*, vol. 182, no. 3-4, pp. 625–631, 2015.

[17] Y. L. Cui, H. Chen, D. Tang, H. Yang, and G. Chen, "Au(III)-promoted polyaniline gold nanospheres with electrocatalytic recycling of self-produced reactants for signal amplification," *Chemical Communications*, vol. 48, no. 83, pp. 10307–10309, 2012.

[18] Y. L. Cui, H. Chen, L. Hou et al., "Nanogold-polyaniline-nanogold microspheres-functionalized molecular tags for sensitive electrochemical immunoassay of thyroid-stimulating hormone," *Analytica Chimica Acta*, vol. 738, pp. 76–84, 2012.

[19] M. M. Nobrega, K. S. Souza, G. F. S. Andrade, P. H. C. Camargo, and M. L. A. Temperini, "Emeraldine salt form of polyaniline as a probe molecule for surface enhanced Raman scattering substrates excited at 1064 nm," *Journal of Physical Chemistry C*, vol. 117, no. 35, pp. 18199–18205, 2013.

[20] T. Wang, T. Xie, and C. Xu, "Microextractors applied in nuclear-spent fuel reprocessing: Micro/mini plants and radiochemical analysis," *Critical Reviews in Environmental Science and Technology*, vol. 49, no. 1, pp. 1–31, 2019.

[21] X. L. Tang, W. Qian, A. Hu, Y. M. Zhao, N. N. Fei, and L. Shi, "Adsorption of thiophene on Pt/Ag-supported activated carbons prepared by ultrasonic-assisted impregnation," *Industrial & Engineering Chemistry Research*, vol. 50, no. 15, pp. 9363–9367, 2011.

[22] K. K. Pandey, "A Study of chemical structure of soft and hardwood and wood polymers by FTIR spectroscopy," *Journal of Applied Polymer Science*, vol. 71, no. 12, pp. 1969–1975, 2015.

[23] G. Pilate, B. Chabbert, B. Cathala et al., "Lignification et bois de tension," *Comptes Rendus Biologies*, vol. 327, no. 9-10, pp. 889–901, 2004.

[24] Y. T. Long, H. Li, Z. du, M. Geng, and Z. Liu, "Confined Gaussian-distributed electromagnetic field of tin(II) chloride-sensitized surface-enhanced Raman scattering (SERS) optical fiber probe: From localized surface plasmon resonance (LSPR) to waveguide propagation," *Journal of Colloid and Interface Science*, vol. 581, Part B, pp. 698–708, 2021.